Proceedings of the 5th International Conference on Nanotechnology: Fundamentals and Applications
Prague, Czech Republic, August 11-13, 2014
Paper No. 80

Solution of the Schrödinger Equation for Strong and Weak Particle Confinement inside a Triangular Quantum Dot

Yuri Vorobiev
Centro de Investigación y de Estudios Avanzados del IPN (CINVESTAV) Querétaro,
2000 Libramiento Norponiente, Fracc. Real de Juriquilla, Querétaro, Mexico 76230
yvorobiev@qro.cinvestav.edu.mx

Vítor Rocha Vieira
Centro de Física das Interacções Fundamentais (CFIF), Instituto Superior Técnico,
Universidade Técnica de Lisboa, Avenida Rovisco Pais, Lisbon, Portugal 1049-001
vrv@cfif.ist.utl.pt

Paul Horley and Jesús González Hernández
Centro de Investigación en Materiales Avanzados, S.C. (CIMAV), Chihuahua/Monterrey,
120 Avenida Miguel de Cervantes, Chihuahua, Mexico 31109
paul.horley@cimav.edu.mx; jesus.gonzalez@cimav.edu.mx

Abstract **-**The present paper addresses solution of the Schrödinger equation in triangular-shaped quantum dots using even and odd mirror boundary conditions corresponding to the cases of strong and weak confinement. We illustrate the fundamental difference between quantum confinement types for two-dimensional triangular-shaped quantum dot, presenting probability distribution plots showing localization of the particle and main tunneling channels (when applicable) at the borders of the quantum dot.

Keywords**:** Schrödinger equation, Quantum dot, Quantum tunnelling, Mirror boundary conditions.

1. Introduction

The recent advances in nano-technology were achieved after significant improvement of theoretical description of nano-structures and corresponding quantum-mechanical phenomena. The considerable interest is focused over nano-particles of different shapes that are widely used in photovoltaic and optical devices (Watanabe et al., 2004; Karl et al., 2008), semiconductor industry (Green, 1998), and bio-medical applications (Torchynska and Vorobiev, 2011). The most common treatment of the problem of a confined particle consists in assumption of strong confinement approximation (Gaponenko, 1998), aiming on calculation of energy levels of a confined particle (either electron or exciton) and determination of the areas inside the quantum dot where the particle could be located in accordance with the set of corresponding quantum numbers.

However, some experimental studies (see, for example, Dabbousi 1977) have shown that the approximation of strong quantum confinement is not entirely accurate in the cases when quantum tunneling is possible through the potential barriers that delimit a quantum dot. This confinement is called weak quantum confinement (Vorobiev et al., 2012) and it becomes even more prominent in the case when several quantum dots are neighboring, creating a kind of periodic structure, which can be especially true for the systems with poor dispersion of nano-particles. If we consider nano-particles made of the same material, deposited over a substrate or submerged into another material, it becomes obvious that in event of touching nano-particles an electron confined in one nano-object would have more ease to tunnel into another nano-object made of the same material rather than tunneling through to a with drastically

different properties. It goes without saying that such tunneling may have an important influence over parameters of nano-particle clusters, and should receive a detailed theoretical study.

However, an explicit analytical treatment of quantum tunneling in a system of multiple quantum dots is considerably complicated (Gaponenko, 1998). Therefore, it is timely and important to search for a robust approximation that can provide good estimation for the properties of nano-particle clusters that may involve weak quantum confinement and tunneling. In particular, we will focus on triangular-shape quantum dots corresponding to the molecules of organic dye erythrosine (Vorobiev and Torchynska, 2010). It should be added that, according to our preliminary results, the energy spectra of a triangular quantum dot and a pyramid with triangular base are considerably similar, which suggests possible applicability of the results described below also to experiments focusing on pyramidal quantum dots.

2. Theoretical Model

Let us consider a two-dimensional quantum dot of triangular shape situated in *x*-*y* plane. By introducing the basis vectors for direct and reciprocal lattices (see for details Vieira et al., 2008) it is possible to obtain the periodic wave functions of the form $\Psi = \exp(i\mathbf{kx})$ with $\mathbf{k} = 2\pi p_i \mathbf{a}^i$, where p_i are quantum numbers describing the state of the particle and $\mathbf{a}^i$ are the vectors of reciprocal lattice:

$$\mathbf{a}^1 = \frac{1}{3}\left(\frac{\sqrt{3}}{2}\mathbf{i} - \frac{1}{2}\mathbf{j}\right), \qquad \mathbf{a}^2 = \frac{1}{3}\left(\frac{\sqrt{3}}{2}\mathbf{i} + \frac{1}{2}\mathbf{j}\right). \tag{1}$$

The energy corresponding to such wave vector **k** can be given as

$$E = \frac{2h^2}{9ma^2}(p_1^2 + p_1 p_2 + p_2^2). \tag{2}$$

It was shown in Ref. (Vorobiev and Torchynska, 2010) that the energy spectrum of erythrosine molecule agrees with Equation (2). It should be emphasized that this expression has no adjustable parameters, defining energy spectrum essentially with molecule's dimensions. Besides, the energy spectra of a particle confined in pyramid-shape quantum dot of the similar size (Vorobiev et al., 2013) feature similar energy scale, in agreement with observation above.

To solve the Schrödinger equation for a confined particle, it is necessary to specify the boundary conditions. Here, we would like to illustrate the use of "mirror" boundary conditions that represents the boundaries of a quantum dot as mirrors reflecting the wave packets corresponding to the confined particle (Vorobiev et al., 2010). Upon such reflection, the wave function of the particle will form a system of standing waves inside the quantum dot. This periodic structure can be constructed by equaling the values of the wave function in a certain point inside the dot (the "object" point) with that in the point obtained as a reflection in a plain mirror aligned with the boundary of the quantum dot (the "image" point).

It should be noted, however, that as the physical meaning of the wave function – the probability to find the particle in the given volume – is connected with the product $\Psi^*\Psi$, which will remain the same even upon permutation of wave function sign. Therefore, when equaling the wave function in "object" and "image" points in respect to reflecting boundary, it is possible to consider the case $\Psi_{object} = -\Psi_{image}$ or $\Psi_{object} = \Psi_{image}$, resulting in odd and even mirror boundary conditions. The former will describe the case of strong quantum confinement with wave function vanishing at the boundary, and the latter – the case of weak quantum confinement with the wave function permitted to have non-zero values at the boundary, which thus will include a certain probability of tunneling.

Applying even and odd boundary conditions to the wave function constructed for triangular quantum dot, one obtains the following odd-function solution:

$$\Psi_{Re} = \cos(k_x u + k_y v) - \cos(k_x u + k_y t) - \cos(k_y u + k_x v) + \cos(-k_y u - k_x t) + \cos(-k_x v + k_y t) - \cos(k_y v - k_x t), \quad (3)$$

$$\Psi_{Im} = \sin(k_x u + k_y v) - \sin(k_x u + k_y t) - \sin(k_y u + k_x v) + \sin(-k_y u - k_x t) + \sin(-k_x v + k_y t) - \sin(k_y v - k_x t). \quad (4)$$

For the case of even boundary conditions the solutions of Schrödinger equations are:

$$\Psi_{Re} = \cos(k_x u + k_y v) + \cos(k_x u + k_y t) + \cos(-k_y u - k_x v) + \cos(-k_y u - k_x t) + \cos(-k_x v + k_y t) + \cos(k_y v - k_x t), \quad (5)$$

$$\Psi_{Im} = \sin(k_x u + k_y v) + \sin(k_x u + k_y t) + \sin(-k_y u - k_x v) + \sin(-k_y u - k_x t) + \sin(-k_x v + k_y t) + \sin(k_y v - k_x t), \quad (6)$$

where the following new variables were introduced:

$$t = \frac{1}{2} - \frac{2}{3\sqrt{3}} y, \quad u = \frac{1}{6} + \frac{1}{3\sqrt{3}}(x - y), \quad v = \frac{1}{6} + \frac{1}{3\sqrt{3}}(x + y). \quad (7)$$

3. Calculation Results and Discussion

To study the character of wave function components and probability distribution for a confined particle, we performed calculations using Equations (3-4) and (5-6) for the odd and even boundary conditions. The wave function components were evaluated in each point of uniformly-spaced grid of 800×800 points. The surface visualization was performed with floating horizon method (Mukherjee 2006); the algorithm was expanded for visualization of the underside of the surfaces. To improve the appearance of the images, we performed bilinear interpolation of the data (Buss 2003). To highlight different slopes of the wave function plots, elementary shading was added as a gradient of wave function along the *x*-axis. It is necessary to stress that the integral of $|\Psi|^2$ over nan-particle volume has to yield unity as a probability to locate a confined particle inside the quantum dot. To simplify comparison between different solutions, the surface plots were normalized to keep the same height of the peaks. The normalization coefficient constant for the same combination of quantum numbers to facilitate comparisons. To emphasize the behavior of wave function and probability distribution at the boundary of the quantum dot, we clipped the calculated data with a triangular mask.

Let us focus first on the case of odd boundary conditions, when the wave function vanishes at the boundary in both even and odd cases. Several characteristic plots of the wave function components are given in Figure 1 together with corresponding probability density distribution $|\Psi|^2$. As one can see from the figure, for equal wave numbers $p_1 = p_2 = 1$ the real component Ψ_{Re} vanishes for every coordinate (Fig. 1a). The imaginary component defines the probability distribution that has a maximum at the centre of the dot, characteristic for the ground state.

Increasing quantum numbers to $p_1 = 1$ and $p_2 = 4$, one can see that real and imaginary parts of wave function behaves in a completely different manner (Fig. 1b). The area of the quantum dot is sectioned with straight segments of $\Psi_{Re} = 0$ coinciding with medians of the triangle. The wave function has either maximum or minimum in the centres of the resulting subdivisions. Now, for the imaginary part the

sectioning is done by curves $\Psi_{Im} = 0$ that are perpendicular to the sides of the triangle, which results in non-triangular subdivisions. The probability distribution is characterized with two peaks along each side of the triangle and a larger peak in its centre.

For $p_1 = 2$ and $p_2 = 3$ the subdivision pattern becomes more complicated (Fig. 1c). The Ψ_{Re} features subdivision by a median *and* a curve that is perpendicular to the median and the base of the triangle. The imaginary part is sectioned by curves $\Psi_{Im} = 0$ perpendicular to two sides of the triangle, but there is no curve that touches the third side. The corresponding probability distribution is characterized with three high peaks located in the vicinity of the corners of the triangle; the probability to find the particle in the centre of the quantum dot vanishes. For the excited state with $p_1 = 4$ and $p_2 = 8$ (Fig. 1d) one can see more complicated subdivision pattern formed by the curves $\Psi_{Re} = 0$ and $\Psi_{Im} = 0$, which, however, is strongly related to the case illustrated in Fig. 1c. That is, the triangle is subdivided in four by the straight segment radiating from the centre of each side at an angle $\pi/3$ from each other. Each four sub-triangles essentially replicate the picture seen for $p_1 = 2$ and $p_2 = 3$, with the resulting probability density plot featuring peaks near the corners of every sub-triangle. Therefore, the quantum states depicted in Fig. 1 a-d it show a considerable variety of preferred particle locations, which either shows a peak in the centre of the quantum dot (Fig. 1a, b) or in the vicinity of the corners of the dot (Fig. 1c) or corners of the corresponding sub-divisions (Fig. 1d). It goes without saying that such significant difference of probability distributions defined by the combination of quantum numbers will have considerable influence on the properties of the system.

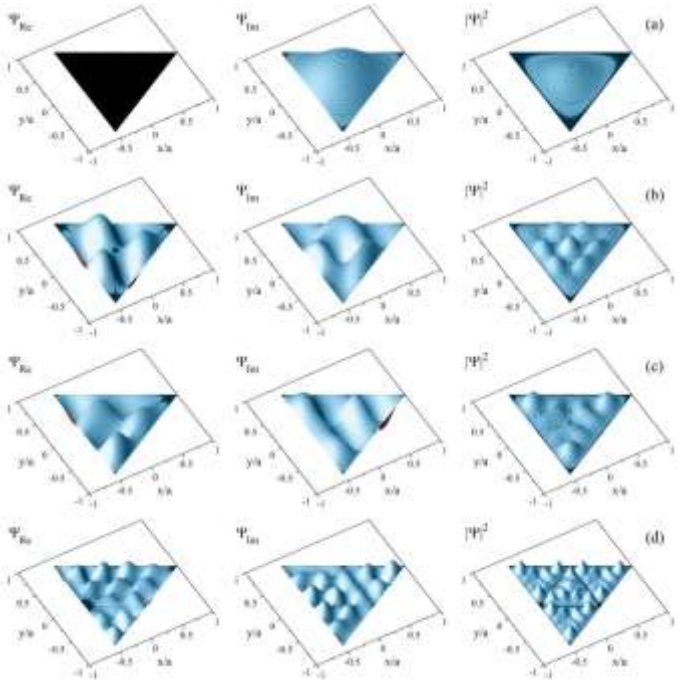

Fig. 1. Surface plots of wave function components Ψ_{Re}, Ψ_{Im} and probability density $|\Psi|^2$ for a particle confined in a triangular quantum dot. The wave function is obtained by solving the Schrödinger equation with odd mirror boundary conditions for the quantum numbers: a) $p_1 = 1$, $p_2 = 1$; b) $p_1 = 1$, $p_2 = 4$; c) $p_1 = 2$, $p_2 = 3$; d) $p_1 = 4$, $p_2 = 8$.

To simplify comparisons, we calculated the distributions of wave function and probability density for the same set of quantum numbers for the case of Schrödinger equation solved with even mirror boundary conditions (Fig. 2). As one can see from the figure, in contrast with the odd boundary solution, for the equal quantum numbers $p_1 = 1$ and $p_2 = 1$ the imaginary part of the wave function vanishes (Fig. 2a). The real part thereof has a shallow minimum in the centre of the quantum dot; the corners of the triangle are marked with considerable maxima of Ψ_{Re}, which dominate the particle probability density landscape (Fig. 2a). Therefore, it is expected that in the system composed of triangular quantum dots fulfilling the

condition of weak quantum confinement, the preferred tunnelling channels will be located at the corners of a triangle.

Upon increasing quantum numbers to $p_1 = 1$ and $p_2 = 4$, the wave function plots undergo sectioning with curves and segments marked with $\Psi_{Re} = 0$ and $\Psi_{Im} = 0$. However, in contrast to Fig. 1, it is clearly seen that sub-division of a triangle with straight segments coinciding with medians occurs more prominently for imaginary part of wave function, while area subdivision with curves perpendicular to the sides of the triangle takes place predominantly for the real part thereof. The corners of the triangle in all cases illustrated in Fig. 2 coincide with extremes of Ψ, producing probability peaks dominating the $|\Psi|^2$ landscape - that is, "pinning" the tunnelling channels to the corners of the triangle. At the same time, a number of probability peaks appearing along the edges of the triangle suggest that under excitation (corresponding to the larger values of p_1 and p_2) additional narrow tunnelling channels open.

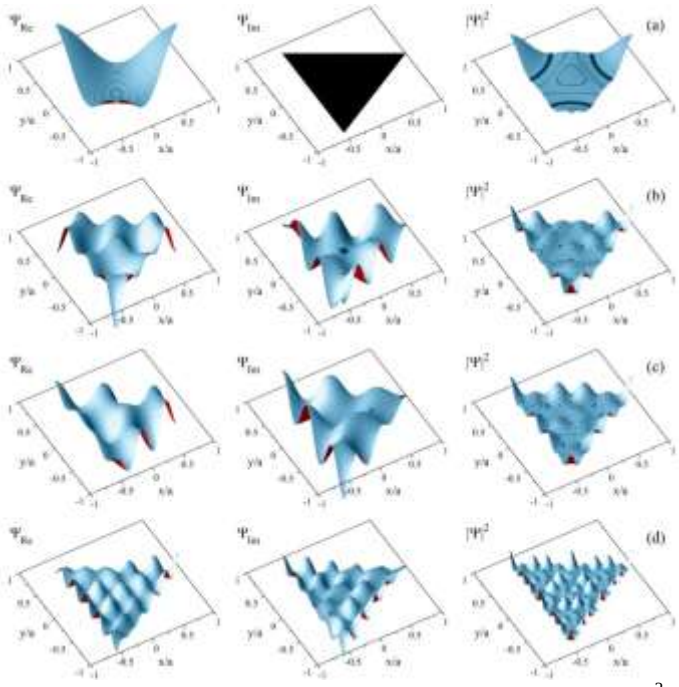

Fig. 2. Surface plots of wave function components Ψ_{Re}, Ψ_{Im} and probability density $|\Psi|^2$ for a particle confined in a triangular quantum dot. The wave function is obtained solving the Schrödinger equation with even mirror boundary conditions for quantum numbers: a) $p_1 = 1$, $p_2 = 1$; b) $p_1 = 1$, $p_2 = 4$; c) $p_1 = 2$, $p_2 = 3$; d) $p_1 = 4$, $p_2 = 8$.

For $p_1 = 2$ and $p_2 = 3$ (Fig. 2c) one can observe formation of two tunnelling channels located near the centre of each side of the triangle. Increasing quantum numbers to $p_1 = 4$ and $p_2 = 8$ (Fig. 2d) adds many new probability peaks along each side and at interior of the quantum dot. We consider this result important, as it suggests that a weakly-confined particle in low-energy states "prefers" to tunnel through wide channels opening at the corners and sides of a triangular quantum dot, which is illustrated with wide probability peaks seen at the boundary (Fig. 2a-c). However, when the energy of the particle grows, the width of the peaks corresponding to tunnelling phenomena significantly reduces; at the same time, multiple probability peaks emerge in the interior of the quantum dot (with the amplitudes comparable to the peaks at the boundary) reflecting the increased degree of particle's localization inside the quantum dot. These results may have significant implications for large periodic systems formed by adjacent triangular quantum dots.

4. Conclusion

We compare odd and even mirror boundary conditions for solution of the Schrödinger equation describing a particle in a triangular-shaped nano-structure. The obtained analytical expressions illustrate

considerable difference between the real and imaginary parts of wave functions corresponding to two-dimensional triangular system. It was shown that probability density plots can be used as a tool to outline the main tunnelling channels in weak confinement case. One of the important conclusions of the analysis is that a particle with a low energy "prefers" tunnelling; at the same time, the excited weakly-confined particle becomes more localized inside the quantum dot.

Acknowledgements

This research was carried out under partial financial support of CONACYT México, grant #152513.

References

Buss, S.R. (2003). "3D Computer Graphics: A Mathematical Introduction with OpenGL" Cambridge University Press.

Dabbousi B.O., Rodriguez-Viejo J., Mikulec F.V., Heine J.R., Mattoussi H., Ober R., Jensen K.F., Bawendi M.G. (1977). (CdSe)ZnS Core-Shell quantum dots: synthesis and characterization of a size series of highly luminescent nanocrystallites. J. Phys. Chem. B. 101, 9463-9475.

Gaponenko S.V. (1998). "Optical Properties of Semiconductor Nanocrystals", Cambridge University Press.

Green M.A. (1992) "Solar Cells: Operating Principles, Technology and System Applications", Prentice-Hall.

Horley P., Vorobiev Yu., Vieira V.R. (2013). Theoretical description of cylindrical nano-structures, including pores in semiconductors, Physica E, 51, 29-36.

Karl M., Weber F.M., J. Lupaca-Schomber, Li S., Passow T., Löffler W., Kalt H., Hetterich M. (2008). GaAs pyramids on GaAs/AlAs Bragg reflectors as alternative microcavities, Superlattices and Microstructures, 43, 635-638.

Mukherjee D.P. (2006). "Fundamentals of Computer Graphics and Multimedia", Prentice Hall.

Torchynska T.V., Yu.V. Vorobiev Y.V. (2011). Semiconductor II-VI Quantum Dots with Interface States and Their Biomedical Applications, in "Advanced Biomedical Engineering" (G.D. Gargiulo and A. McEwan, editors), Intech, Rijeca, Croatia, pp. 143-182.

Vieira V.R., Vorobiev Yu.V., Horley P.P., Gorley P.M. (2008). Theoretical description of energy spectra of nanostructures assuming specular reflection of electron from the structure boundary, Physica Status Solidi C, 5, 3802-3805.

Vorobiev Y.V., Torchynska T.V. (2010). Optical Properties of Nanostructured Materials, in "Nanocrystals and Quantum Dots of Group IV semiconductors", edited by T.V. Torchynska and Yu. V. Vorobiev, American Scientific Publishers, pp. 188-224.

Vorobiev Y.V., Torchynska T.V., Horley P.P. (2013). Effect of aspect ratio on energy of optical transitions in a pyramid-shaped quantum dot. Physica E, 51, 42-47.

Vorobiev Y.V., Mera B, Vieira V.R., Horley P.P., González-Hernández J. (2012). Weak and Strong confinements in prismatic and cylindrical nanostructures, Nanoscale Research Letters, 7, 371.

Vorobiev Y.V., Gorley P.M., Vieira V.R., Horley P.P., González-Hernández J., Torchynska T.V., Diaz Cano A. (2010). Effect of boundary conditions on the energy spectra of semiconductor quantum dots calculated in the effective mass approximation, Physica E, 42, 2264-2267.

Watanabe S., Pelucci E.,, B. Dwir B., Baier M.H., Leifer K., E. Kapon E. (2004). Dense uniform array of site-controlled quantum dots grown in inverted pyramids. Appl. Phys. Lett., 84, 2907-2909.